EXPERIMENTAL AND NUMERICAL PREDICTION OF SURFACE CRACK GROWTH IN FATIGUE IN A FINITE WIDTH PLATE

S. K. Patel*, B. Dattaguru** and K. Ramachandra*

Abstract

In the thick components such as gas turbine disks, the cracks usually manifest in the form of part-through or embedded elliptical cracks. The shape of surface crack varies during the crack propagation and significantly affects the fatigue life predictions of the surface cracked components. In present work, crack propagation of semi-elliptical cracks in a finite width specimen of a gas turbine material subjected to fatigue load has been studied experimentally and numerically. The numerical simulation was accomplished by first extending the applicability of available stress intensity factor empirical equation for semi-elliptical cracks to finite width solid. Using this empirical equation for stress intensity factor, the effect of change in the crack shape on the crack propagation life is simulated by numerical models. Also, in order to include the effect of crack closure in the numerical prediction of growth of surface cracks, a ratio of crack closure factor between depth and surface locations of a semi-elliptical crack was obtained by experiments. The experimental observations were used in correlating the numerical predictions for crack shape progression and crack propagation life.

Introduction

Design based on damage tolerance concepts has become mandatory in high technology structures. These concepts are also essential for life extension of aged structures which are in service beyond originally stipulated life. In the thick components such as gas turbine disks, the cracks usually occur in the form of part-through or embedded elliptical cracks.

In the literature [1-13] a large amount of testing and analysis concerning the growth of surface cracks during fatigue growth has been performed. Some of these results for semi-elliptical cracks in tension and bending plates have been summarised by Hosseini and Mahmoud [14]. The studies reported in literature are concerned with a semi-elliptical crack in a wide plate. Usually, the crack shape development model relies on the availability of close or empirical form stress intensity factor solution for the configuration. The Newman-Raju [15] empirical solution for semi-elliptical crack subjected to tension is used in this model because of its accuracy. However, this solution for the semi-elliptical crack is valid only for $a/t < 1.0$, $a/c = 0$ to 2 and $c/W < 0.5$. Hence, the simulations reported in the literature are upto crack width (c) less than half of the width of the plate (W). The specimen considered in the present study, which is also recommended by AGARD [16] and representative of finite width of typical gas turbine disks, has width equal to half of its thickness. In such a specimen during the crack propagation, the c/W (crack length on surface to specimen width) may violate the limitation on c/W (< 0.5) of the Newman-Raju stress intensity factor solutions for semi-elliptical crack and thus can not be used in full range of crack growth. Therefore, in the present work the validity of Newman-Raju [15] solution is extended upto crack to specimen width (c/W) upto 0.9 in order to simulate the crack growth in finite width plate. This is enabled by first obtaining the stress intensity factors solutions in the range of $c/W = 0.5$ to 0.9 ($c/W = 0.5$, 0.6, 0.7, 0.8 and 0.9) for various aspect ratios $a/c = 0.2$, 0.4, 0.6, 0.8, 1.0 and 2.0. Based on these solutions, a modified finite width correction is proposed which can directly be used along stress intensity factor solution for semi-elliptical crack developed by Newman-Raju [15]. Subsequently, this solution is used in fatigue crack growth study of single semi-elliptical crack in a finite width solid.

* Scientists, Gas Turbine Research Establishment, CV Raman Nagar, Bangalore-560 093, India
** Department of Aerospace Engineering, Indian Institute of Science, Bangalore-560 012, India

Original paper presented during the XI National Seminar on Aerospace Structures (XI NASAS) held on 8-9 February 2002 at National Aerospace Laboratories, Bangalore, India

Revised paper received on 11 Mar 2005; Paper accepted on 17 Mar 2005

In present work, crack shape development vis-a.-vis crack propagation life of semi-elliptical crack in a finite width solid subjected to tension load has been studied experimentally and numerically. The modified empirical equation for stress intensity factor for semi-elliptical crack to account the effect of finite width, as developed in this work, is employed in the numerical simulation. The surface crack specimens of aero-engine disk material Inconel-718 are tested under uniaxial fatigue loading. The PPP (Preferred Propagation Path) is predicted for semi-elliptical crack in a finite width solid and compared with that of a crack in wide plate. The crack shape development is predicted by two degrees and multi degrees of freedom models. Also the effect of crack closure on the crack shape evolution is included in the numerical models by obtaining the crack closure levels at surface and deepest points of the crack by front and back face strain gauges respectively. The experimental observations on the crack shape development and crack propagation life in the finite width specimen are further used in evaluating the numerical tools developed in this work for fatigue crack growth simulation of surface cracks.

Crack Propagation Model

The change in shape of surface crack during fatigue loading can be predicted using semi-analytical/numerical and computational models. The "semi-analytical method" relies on empirical form of stress intensity factor solution and the shape of the crack at various stages of growth is determined by two degrees of freedom. Although "semi-analytical method" restricts the crack shape to be only elliptical or circular but it is computationally inexpensive.

In order to predict aspect ratio changes during fatigue crack growth using local stress intensity factor based semi-analytical model, a number of assumptions are made as listed below:

- The fatigue crack will grow in a semi-elliptical shape i.e. determination of the semi-minor and major axes at any stage of growth will be sufficient in defining the crack front.
- Crack growth rate at the ends of the semi-elliptical crack will be assumed to be dependent on the value of the local SIF only.
- The material is assumed to be homogeneous and isotropic.
- Paris crack-growth equation is assumed to be valid.

Numerous studies [1-14] on the evolving shape of surface cracks in fatigue are reported in literature. All these studies are in general based on Paris equation. The Paris equation for prediction of crack growth rate for three-dimensional crack can be written in the following generalised form

$$\frac{da_i}{dN} = f(\Delta K_i, C_i, n_i) \tag{1}$$

where ΔK_i is discrete stress intensity factor range at "ith degree of freedom", "N" is the number of load cycles, "C_i" and "n_i" are material constants of Paris equation, "i" is the degree of freedom, a_i is the characteristic dimension at ith degree of freedom. Here, infinite degrees of freedom of surface crack are reduced to finite degrees of freedom. Usually, two degrees of freedom (DOF) are sufficient to describe elliptical or circular crack front growth used in the eq.(l) based on the assumption (1) mentioned above. These two DOF are two principal dimensions of an ellipse. The equations for the crack growth in 'a' and 'c' can be written as

$$\frac{da}{dN} = C_a (\Delta K_a)^{n_a} \tag{2}$$

$$\frac{dc}{dN} = C_c (\Delta K_c)^{n_c} \tag{3}$$

Where C_a , C_c and n are material properties, K_a and K_c are the values of stress intensity factor at points 'A' ($\varphi = 90$) and 'C' ($\varphi = 0$) respectively as shown in Fig.1.

Using eqs. (2) and (3) and assuming n_a and n_c equal to n, the equation for crack shape development can be written as

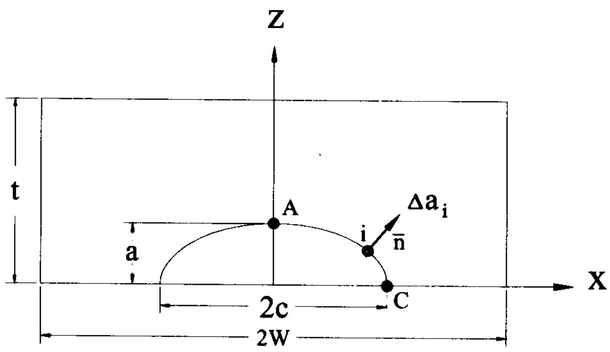

Fig.1 Basic geometric parameters of semi-elliptical surface

$$\frac{dc}{da} = \frac{C_c}{C_a}\left(\frac{\Delta K_c}{\Delta K_a}\right)^n \qquad (4)$$

Assuming, the material constants "n" and "C" are independent of spatial location on the crack front, eq.(4) can be written as

$$\frac{dc}{da} = \left(\frac{\Delta K_c}{\Delta K_a}\right)^n \qquad (5)$$

Adopting the plasticity induced closure concept, the conventional crack growth equation using stress intensity factor ranges may be modified to incorporate the effects of plasticity induced crack closure as follows:

$$\frac{dc}{da} = \left(\frac{U_C\,\Delta K_c}{U_A\,\Delta K_a}\right)^n \qquad (6)$$

Where U_C and U_A are Elber crack closure factor at crack front locations 'A' and 'C' respectively.

By introduction of factor β_R, which is defined as the ratio of crack closure factor at 'C' and 'A', eq.(6) can be written as

$$\frac{dc}{da} = \left(\beta_R \frac{\Delta K_c}{\Delta K_a}\right)^n \qquad (7)$$

Jolles and Tortoriello [2] assumed $\beta_R = 0.911$. A similar value (an empirical factor) equal to 0.9 was suggested by Newman and Raju [15] in the Paris equation for surface crack i. e. eq.(4) assuming that $C_c = (0.9)^n C_a$. It should be noted here that the factor equal to 0.9 suggested earlier by Newman and Raju [15] was not to account for differences in crack closure but to account for different crack growth resistance at the surface and at the deepest point on the semi-elliptical crack.

The *da*/*dN* rate, *da*/*dc* and range of stress intensity factor (ΔK) are numerically integrated to determine the crack size and shape as a function of cyclic life. In numerical simulation of surface cracks Δa is taken equal to 0.001 of a_o. The flow chart of the analysis is shown in Fig.2.

Two degrees of freedom ("a" and "c" for a semi-elliptical crack model) model along with close form stress intensity factor solutions has been used in the present work. The empirical solutions (fitted equations for stress intensity factor from finite element solutions) provided by Newman- Raju [15] are used with finite width correction as proposed in the present work. A "multi-DOF model" is also used in predictions of crack shape development. The basic steps involved in multi-DOF are identical to two degrees of freedom model except the crack is grown at multi points on the crack front and subsequently the new crack front is fitted in ellipse shape using the least square technique.

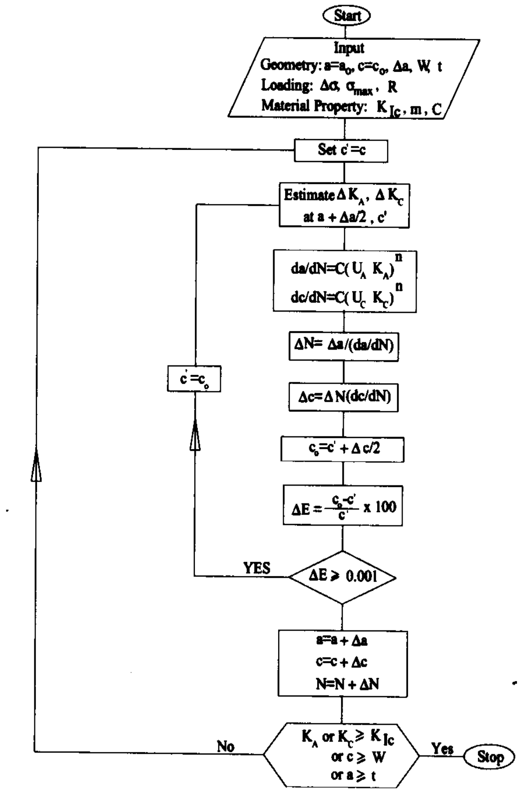

Fig.2 Flow diagram for fatigue growth simulation of surface crack

Finite Width Correction

Newman and Raju [15] formulated an empirical equation to estimate the stress intensity factors for a wide variety of parameters for the semi-elliptical crack subjected to tension and also an empirical equation was developed from the stress intensity factors obtained from finite element analyses. The equation for stress intensity factor was written in the following form

$$K = \sigma\sqrt{\left(\frac{\pi a}{Q}\right)}\; F\left(\frac{a}{t}, \frac{a}{c}, \frac{c}{W}, \varphi\right) \qquad (8)$$

Where

$$F = \left[M_1 + M_2\left(\frac{a}{t}\right)^2 + M_3\left(\frac{a}{t}\right)^4\right] g f_\varphi \, f_w$$

The function 'Q' is the shape factor for an ellipse and is given by the square of the complete elliptical integral of the second kind. The boundary correction factor is a function of crack depth, crack length, plate thickness, plate width and parametric angle of the ellipse. The series containing 'M_i' are the boundary correction factors at the maximum depth point (φ = 90). The function f_φ is an angular function derived from the solution for an elliptical crack in an infinite solid. This function accounts for most of the angular variation in stress intensity factors. The function 'g' is used to fine-tune the equation. The function 'f_w' is a finite width correction.

Newman-Raju [17] solution of semi-elliptical crack subjected to tension has the following range of applicability:

Parametric angle (φ)	a/t	a/c	c/W
0-π	<1.25 (a/c+0.6) for 0≤a/c ≤ 0.2 and < 1 for a/c > 0.2	0 to 2	< 0.5

In the above Newman-Raju stress intensity factor solution, the limitation on c/W < 0.5 is most stringent, particularly for the specimen having W = t/2 as adopted in gas turbine materials characterization programme [16]. In the present work stress intensity factors in the range of c/W between 0.5 to 0.9 for a/c=0.2, 0.4, 0.6, 0.8, 1.0 and 2.0 have been obtained using finite element analyses. The tabular SIF $\left(K_I \Big/ \frac{\sigma\sqrt{\pi a}}{Q}\right)$ solution is given in reference [18]. In all the analyses, Poisson's ratio is assumed to be 0.3. The stress intensity factors are estimated using MVCCI (Modified Virtual Crack Closure Integral) with proposed area and curvature corrections [18].

It is quite clear from Fig.3 that if Newman-Raju solution has to be used for c/W > 0.5 a correction is necessary to account for the effect of finite width. The correction factor should also account for the variation of stress intensity factor along the crack front. Thus in order to account for the effect of finite width (c/W ≥ 0.5), a function f_{w_1} is fitted to the SIF solution based on least square fit as

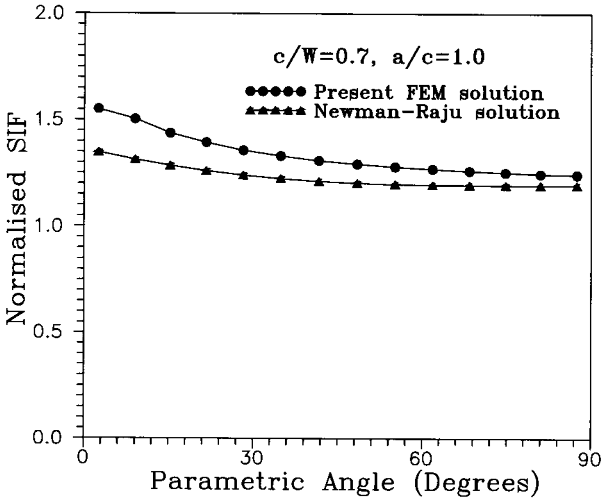

Fig.3 Comparison of present FEM and Newman-Raju [70] SIF solution for semi-elliptical crack of c/W = 0.7 and a/c = 1.0

$$f_{w_1} = 0.98 + 0.065\left(\frac{a}{c}\right)^4 + 0.08\sqrt{\left(\frac{a}{t}\right)}\,(1 - \sin\varphi)\, f_{cw}$$
for a/c ≤ 1.0 (9a)

$$f_{w_1} = 0.98 + 0.065\left(\frac{c}{a}\right)^4 + 0.08\sqrt{\left(\frac{a}{t}\right)}\left(1 - \frac{a}{c}\sin\varphi\right) f_{cw}$$
for a/c > 1.0 (9b)

where

$$f_{cw} = \left[27.6038 - 186.665\frac{c}{W} + 472.059\left(\frac{c}{W}\right)^2 - 526.072\left(\frac{c}{W}\right)^3 + 225.585\left(\frac{c}{W}\right)^4\right]$$

Here, it is proposed that stress intensity factor for finite width (c/W ≥ 0.5) can be estimated using the following modified Newman-Raju equation

$$F = \left[M_1 + M_2\left(\frac{a}{t}\right)^2 + M_3\left(\frac{a}{t}\right)^4\right] g f_\varphi \, f_w \, f_{w_1} \quad (10)$$

Similar to Newman-Raju equation, the present correction is accurate within ±5% of finite element analyses. Fig.4 shows the stress intensity factors variation along the crack front obtained using above proposed eq. (10) with

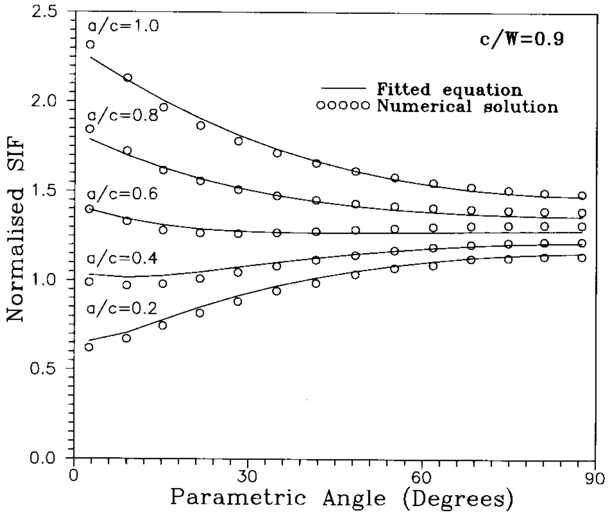

Fig.4 Comparison of numerical and eq.(3.10) stress intensity factor solutions for c/W = 0.9

eq.(9) and finite element analyses for c/W=0.9. It is evident from Fig. 4 that the proposed finite width correction, eqs.(9(a)-(b)) is accurate in representing the variation of stress intensity factor along the crack front. The developed empirical equations for semi-elliptical cracks in finite width plate are found to be within ±5% of the finite element solutions.

Specimen and Testing Procedure

A surface crack specimen with a semi-elliptical crack at the center is considered for testing. The specimen is rectangular in shape in the gauge section having thickness, t, and width, 2W. The major dimensions of the specimen are shown in Fig.5.

The material of specimen selected for present study is Nickel base superalloy Inconel- 718 [19] which is extensively used for components of gas turbine engines, liquid rockets, cryogenic tankage etc. Inconel-718 is a high strength, corrosion resistant material used at -252°C to 705°C. The specimens are made out of rolled bar of 20mm diameter using wire cutting EDM (Electrical Discharge Machining). The specimens were aged after machining. The ageing heat treatment cycle was 720°C/8hrs/furnace cooled at 620°C @ 50°C/hr/8hrs/Aircooled.

Table-1 : Mechanical properties of material at room temperature				
UTS	0.2 PS	RA	Hardness	E [19]
MPa	MPa	%	BHN	MPa
1470	1210	44	331	200039

The material properties of the alloy are listed in Table-1. These material properties were obtained from coupons extracted from the same lot and heat treatment as specimens considered for crack growth study.

The initial flaw, elliptical in shape, was created by EDM method. The geometry of flaw was measured from the fractured specimen after the completion of testing and was found to have crack depth, a = 0.285mm and crack width, 2c = 1.337mm. A scanning electron microscopy picture of one of the typical notches is given in Fig.6.

The test on specimen has been conducted under constant amplitude uniaxial loading at room temperature in air. The maximum applied stress was 674.54 MPa and stress ratio was 0.05. The cycle consists of a loading block, closure detection block [20] and marker blocks. Marker block is used in order to obtain crack shape progression during fatigue testing. The marker block consists of load cycles with the same maximum stress whereas the minimum stress is increased corresponding to stress ratio (R) of value 0.5-0.8. It was observed that the marking block with high stress ratio (R=0.8) gives marking impression of better visibility (or darkness). Crack closure block was applied on the specimen in order to get the crack closure levels from scanning electron microscope. However, the

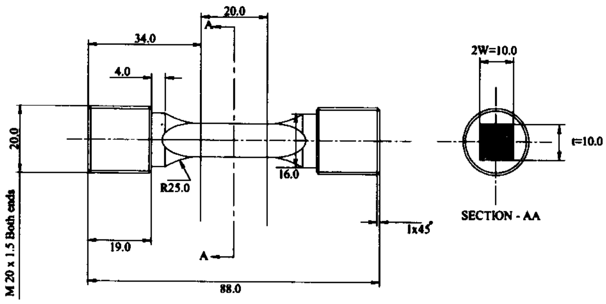

Fig.5 Specimen geometry

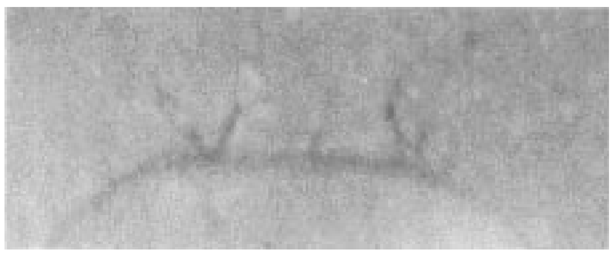

Fig.6 SEM photograph of initial flaw

further processing of closure impression on the specimen could not be carried out. The loading cycle was triangular in waveform having frequency 2Hz. The testing was carried out on MTS Servo-Hydraulic Universal Tensile Testing machine with variable testing capacity upto 50T. The load sequences used in experiments were controlled by a micro-console. The machine was calibrated before start of the testing.

A special gauge called 'KRAK-GAGE' [21] which works on indirect DC potential drop is used in the present work for continuous measurement of the crack length at surface. Small strain gauges were used to monitor strains near the crack tip and on the back face, exactly behind the crack as shown in Fig.7.

Results and Discussions

Measurement of Crack Closure for Semi-Elliptical Crack

In the present work, crack closure levels at surface and deepest points of the crack were measured by front and back face strain gauges respectively. The front face gauge is mounted 2mm ahead of crack tip (crack front at surface) whereas the back face gauge was bonded exactly behind the crack and on the opposite face. The use of near tip and back face gauges for measurement of closure levels on surface crack was demonstrated by Soboyejo et al.[22]. It is reasonable to assume that the measurements from these front and back face strain gauges provide crack closure levels at the crack tips at the surface and at the maximum depth point respectively. In order to record the strains, the test was conducted at very low frequency. The strains were recorded from 'system-4000 [23]', a digital signal conditioner, at certain intervals during the tests. Fig.8 shows the strain derivative function $\left(\left[\left(\varepsilon_i-\varepsilon_{i-1}\right)/\left(P_i-P_{i-1}\right)\right] / \left[\left(\varepsilon_m-\varepsilon_{m-1}\right)/\left(P_m-P_{p-1}\right)\right]\right)$ plotted against the load. The change in the slope of this function

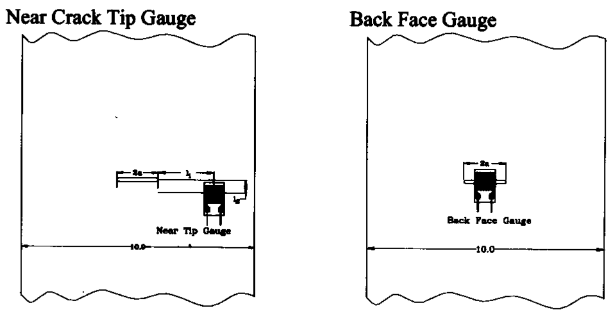

Fig.7 Strain gauge locations

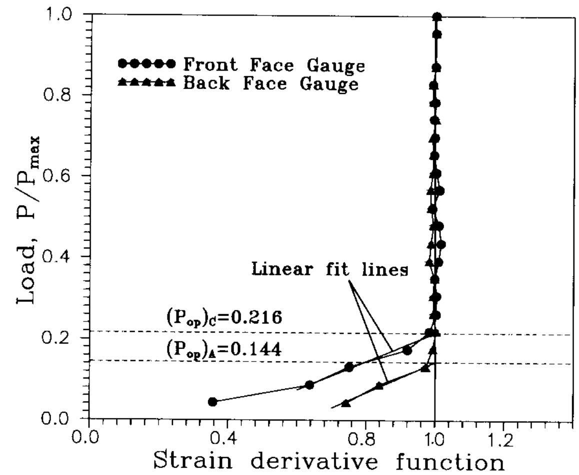

Fig.8 Crack opening levels at locations 'A' (at depth) and 'C' (at surface) for semi-elliptical crack

gives crack opening level. Thus a straight line is fitted to data near the change in slope of strain and where this fitted line intersects with vertical line is assumed the crack opening point and the corresponding load is taken as crack opening load. The crack opening level obtained by near tip gauge is assigned to location 'C' i.e.$\varphi = 0°$ where the backface gauge is expected to represent the crack opening at depth location 'A' i.e.$\varphi = 90°$. The crack opening loads (P_{op}/P_{max}) at surface and depth are found to be 0.216 and 0.144 respectively and corresponding crack closure factor ratio ($\beta_R=U_C/U_A$) found to be 0.9158 for the considered superalloy Inconel-718.

Crack Shape Development and Propagation Life

The crack shapes at various cycle intervals were obtained by macroscopic beachmarks introduced during the test, by changing the minimum load keeping maximum load constant. Fig.9 shows one of the photographs of a fracture surface of a specimen.

For each beachmark (crack front), the coordinates of a number of points were obtained using digitized image. The measured points on each crack front are fitted by an ellipse by least square fit technique. The points near the free surface are not considered since crack usually trails behind near the free surface and usually beachmarks are not very clear. Fig.10 shows the measured points and corresponding fitted ellipse for the specimen AI-7. It is clear from Fig.10 that the crack front assumes a shape very close to an ellipse. Thus it is a reasonable assumption that the crack front remains elliptical during the crack growth. Using the numerical tools developed in this work as de-

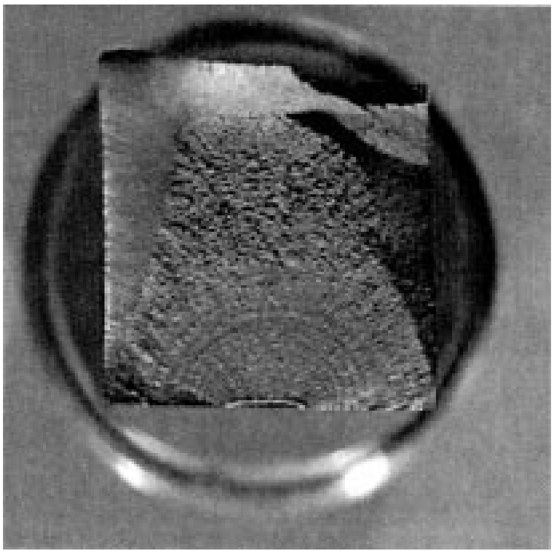

Fig.9 Photograph of fracture surface of specimen (AI-7)

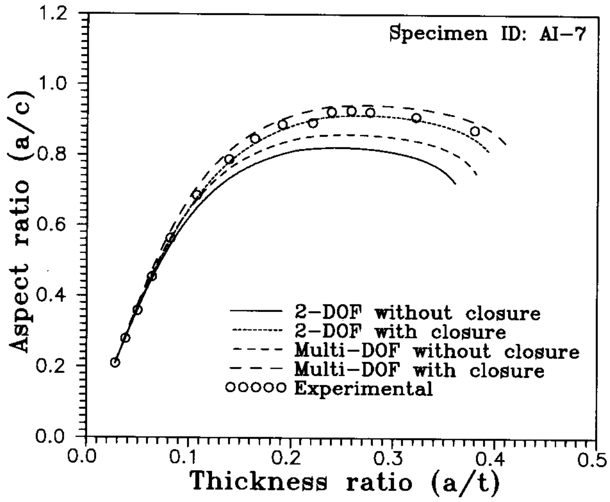

Fig.11 Comparison of experimental and numerically predicted crack shape development for semi-elliptical cracks in finite width specimens

scribed in flow chart, Fig.2, the crack shape development was predicted by both 2-D0F and Multi-DOF models with and without crack closure effects.

The predicted and experimental crack shape development for the initial crack shape is shown in Fig.11. The crack shape change behaviour for semi-elliptical crack in finite width plate has been observed similar to semi-elliptical crack in wide plate [2-6, 12] except at a/t larger than 0.3. In the beginning, crack shape (a/c) changes very rapidly until it reaches approximately a/t = 0.2. The cracks nearly attain a/c = 1.0, subsequently the semi-elliptical

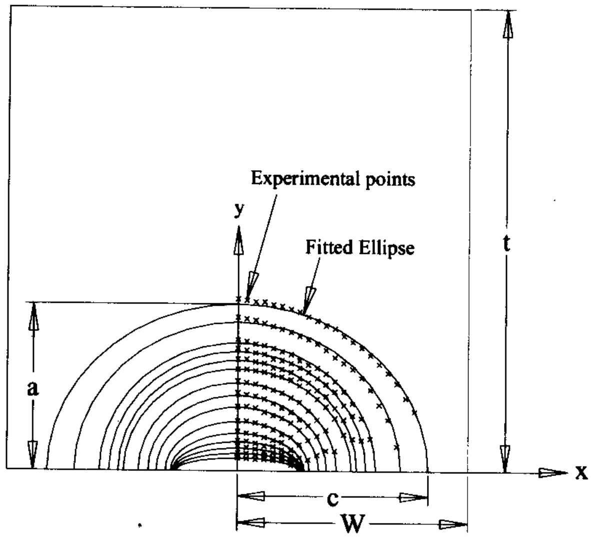

Fig.10 Experimental data points and fitted ellipse for specimen AI-7

cracks in a finite width plate reaches approximately a/t = 0.3, the crack shape decreases significantly with growth of the crack. Similar trends are predicted by numerical simulation of semi-elliptical crack in fatigue by all the four models used in this work. The predictions considering closure (2-DOF or multi-DOF model) compare very well with experimental results for the considered initial crack configuration.

It is noted that by experimental and numerical analyses the crack shape drops faster after a/t = 0.3 for finite width plate. Thus, it is expected that PPP (Preferred Propagation Path) would be different for semi-elliptical crack in a finite width plate. This is demonstrated by a numerical study considering various initial shape semi-elliptical cracks in a finite width plate, t/W = 2 and a wide plate t/W = 0.2. The crack shape development is illustrated in Fig.12. The predicted PPP for semi-elliptical crack in a finite width plate is found to be different compared to that in a wide plate. PPP assumes lower path for semi-elliptical cracks in a finite width plate. This is mainly due to the effect of side faces of specimen, as crack comes in the vicinity of side faces the stress intensity factor increases at location "C" (at surface) more than that at the point "A" (at maximum crack depth). Thus the crack growth rate at location "C" would be higher compared to location "A" and crack starts becoming shallower as it grows.

In estimating the life of a part-though crack, the crack shape evolution plays a major role since the stress intensity factor in part-though crack is not only function of crack length but also the aspect ratio of the crack. The algorithm

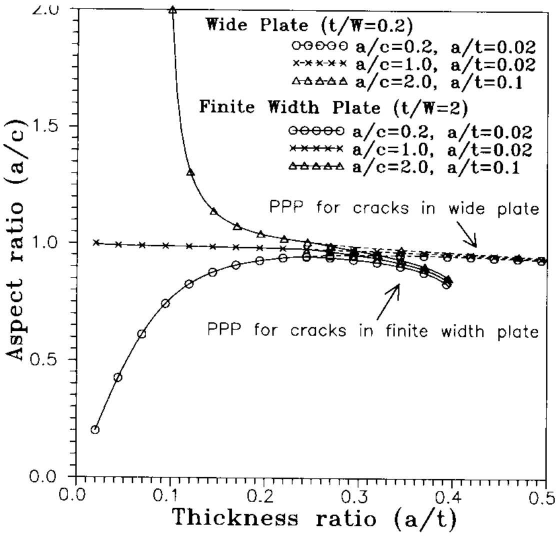

Fig.12 PPP for semi-elliptical cracks in a finite width plate and a wide plate

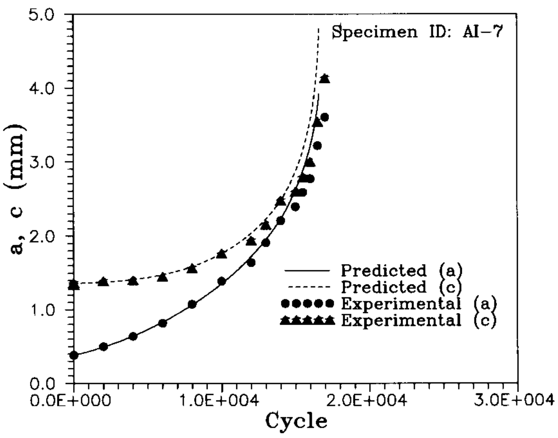

Fig.13 Crack propagation life for the specimen

presented in this paper takes these nonlinear effects into account. The crack propagation life is estimated using the 2-DOF model including Elber closure effects. The crack propagation life is calculated from the first marker rather than the initial notch to eliminate the uncertainty about the initiation life of the notch. The estimated life for the specimen is .compared with experimental results as shown in Fig.13. The ratio of predicted life to experimental life was found to be 0.94 for the specimen (AI- 7).

Concluding Remarks

The empirical form of stress intensity equations for semi-elliptical cracks in finite width plate are developed in this work for c/W upto 0.9. By this the validity of available Newman-Raju stress intensity factor empirical equation for semi-elliptical cracks in finite plate has been extended. The current equations enabled numerical predictions of fatigue crack growth and fatigue life estimations for larger values of c/W (upto 0.9).

The crack shape development from an initial semi-elliptical crack in a finite width plate under fatigue load has been studied by experiments for a gas turbine material Inconel-718. The numerical tools for estimation of the fatigue crack growth and life prediction for semi-elliptical cracks in finite width plate are developed and validated by experiments. These tools have been developed with larger interest towards the damage tolerance design analysis of gas turbine components. The models including crack closure effects compare well with the experimental results. The preferred propagation path for semi-elliptical cracks in finite width plate is obtained. It is observed that the preferred propagation path during fatigue of a semi-elliptical crack in a finite width plate is different compared to a crack in a wide plate. The two degrees of freedom model including closure effects is found to predict the crack propagation life accurately.

References

1. Scott, P. M. and Thorpe, T. W., "A Critical Review of Crack Tip Stress Intensity Factors for Semi-elliptical Cracks", Fat. Fract. Engg. Mater. Struct., Vol.4, pp.291-309,1981.

2. Jolles, M. and Tortoriello, V., "Effects of Constraint Variation on the Fatigue Growth of Surface Flaws", Fracture Mechanics: Fifteenth Symposium, ASTM STP 833, pp.300- 311,1984.

3. Newman Jr. J. C. and Raju, I. S., "Prediction of Fatigue Crack Growth Patterns and Lives in Three-dimensional Cracked Bodies", Advances in Fracture Research, Eds. Valluri S. K., Taplin, D. M. R., Rama Rao, P., Knott, J. F. and Dubey, R., Pragamon Press, Vol. 3, pp.1597-1608, 1984.

4. Jolles, M. and Tortoriello, V., "Geometric Variation During Fatigue Growth of Surface Flaws", Fracture Mech: Fourteenth Symposium Vol.I: Theory and Analysis, ASTM STP 791, Eds. Lewis, J. C. and Shines G., pp.287-307, 1983.

5. Fleck, N. A., Smith, I. F. C. and Smith R. A., "Closure Behavior of Surface Cracks", Fat. Fract. Engg. Mater. Struct., Vol.6, pp.225-239, 1983.

6. Kim, J. and Song, J., "Crack Growth and Closure Behaviour of Surface Cracks Under Axial Loading", Fat. Fract. Engg. Mater. Struct., Vol.15, pp. 477-489, 1992.

7. Muller, H. M., Muller, S., Munz, D. and Neumann, J., "Extension of Surface Cracks During Cyclic Loading", Fracture Mechanics: Seventeenth Volume, ASTM STP-905, Eds. Underwood, J., Chait, R., Smith, C. W., Wilhem, D. B., Andrews W. A. and Newman Jr. J. C., pp.625-643, 1986.

8. Yau, J. F., "An Empirical Surface Crack Solution for Fatigue Propagation Analysis of Notched Components", Fracture Mechanics: Seventeenth Volume, ASTM STP-905, Eds. Underwood, J., Chait, R., Smith, C. W., Wilhem, D. B., Andrews W. A. and Newman Jr. J. C., pp.601-624, 1986.

9. Hodulak, L., Kordisch, M., Kunzelmann. and Sommer, E., "Growth of Part-through Cracks", Fracture Mechanics, ASTM STP 677, Ed. Smith, C. W., pp.399-410, 1979.

10. Van Stone, R. H., Gilbert, M. S., Gooden, O. C. and Laflen, J. H., "Constraint-loss Model for the Growth of Surface Cracks", Fracture Mechanics Symposium, ASTM STP 969, Ed. Cruse T. A., pp.637-656, 1988.

11. Hosseni, A. and Mahmoud, M. A., "Evaluation of Stress Intensity Factor and Fatigue Growth of Surface Cracks in Tension Plates", Engg. Fract. Mech., Vol. 22, pp.957-974, 1985.

12. Shuter, D. M. and Geary W., "Fatigue Crack Growth from Two-dimensional Surface Defects", Fat. Fract. Engg. Mater. Struct., Vol.18, pp. 653-659, 1995.

13. Wilson, C. D., "Fracture Mechanics Life Prediction Computer Code Verification and Validation", Fracture Mechanics; 26th Volume, ASTM STP 1256, Eds. Walter, G. R., Underwood, J. H. and Newman Jr, J. C., pp.779-798, 1995.

14. Mahmoud, M. A., "Quantitative Prediction of Growth Patterns of Surface Fatigue Cracks in Tension Plates", Engg. Fract. Mech., Vol. 30, pp.735-746, 1988.

15. Newman Jr. J. C. and Raju, I. S., "An Empirical Stress Intensity Factor Equation for the Surface Flaw", Engg. Fract. Mech.,Vol.15, pp.185-192, 1981.

16. Raizenne, M. D., "Fatigue Crack Growth Results for Ti-6Al-4V, IMI685, and Ti-17", AGARD Engine Disc Cooperative Test Program, AGARD R-766 (Addendum), 1993.

17. Newman Jr. J. C. and Raju, I. S., "Prediction of Fatigue Crack Growth Patterns and Lives in Three-dimensional Cracked Bodies", Advances in Fracture Research, Eds. Valluri S. R., Taplin, D. M. R., Rama Rao, P., Knott, J. F. and Dubey, R., Pragamon Press, 3: pp.1597-1608, 1984.

18. Patel, S. K., "Experimental and Numerical Studies on Fatigue Crack Growth of Single and Interacting Multiple Surface Cracks", Ph. D. Thesis, Indian Institute of Science, Bangalore, India, May, 2000.

19. Inconel Alloy 718, Technical Bulletin, Inco Alloys International, Inc., 4th Edition, West Virginia, 1985.

20. Seshadri, B.R., Dattaguru, B., Ramamurthy, T. S., Sundar, R. and Prakash, R. V., "Finite Element Simulation and Experimental Correlation of Crack Closure Phenomenon Under Cyclic Loading", J. Aero. Soc. of India, Vol.45, pp.281-292, 1993.

21. KRAK gage and FRACTOMAT Bulletin, TTI Division, Hartrun Corporation, Chaska, MN, USA.

22. Soboyejo, W.O. and Knott, J. F., An Investigation of Crack Closure and the Propagation of Semi-elliptical Fatigue Cracks in QIN (HY80) Pressure Vessel Steel, Int. J. Fat., Vol. 17, pp.577-581, 1995.

23. Software and Executive Unit Reference, Ver.1.1, System-4000, Model 510, Stress Analysis Data System, Instruments Div., Measurements Group Inc., Rayleigh, 1992.